# The Influence of the Capping Layer on the Perpendicular Magnetic Anisotropy in Permalloy Thin Films

Mihai S. Gabor[1], Coriolan Tiusan[1,2], Traian Petrisor, Jr.[1], and Traian Petrisor[1]

[1]Center for Superconductivity, Spintronics and Surface Science, Technical University of Cluj-Napoca, Cluj-Napoca 400027, Romania
[2]Institut Jean Lamour, Lorraine University, Nancy 54395, France

**In this paper, we show that perpendicular magnetic anisotropy can be achieved in polycrystalline $Ni_{80}Fe_{20}$ films on MgO underlayers grown on thermally oxidized Si substrates. The perpendicular magnetic anisotropy is already present in the as-deposited films and preserved after thermal annealing. This paper points out the crucial role of the capping layer on the perpendicular magnetic anisotropy stabilization. By changing the nature of the capping from MgO, V, Nb to Ta, the value of the surface anisotropy constant is increased from $0.3 \pm 0.05$ erg/cm$^2$ in the case of the MgO to $0.79 \pm 0.06$ erg/cm$^2$ in the case of the Ta capping, respectively. For Ta capped samples, the perpendicular magnetization is achieved for $Ni_{80}Fe_{20}$ films with an effective thickness below 1.1 nm.**

*Index Terms*—**Magnetic films, perpendicular magnetic anisotropy, sputter deposition, X-ray diffraction.**

## I. Introduction

FERROMAGNETIC THIN films showing perpendicular magnetic anisotropy (PMA) are of great research interest due to their potential use for perpendicular magnetic recording technology, including bit-patterned media, racetrack, and spin transfer torque magnetic memories [1]–[3]. Conventional PMA materials include the L10 ordered alloys (FePt and CoPt), Co-based multilayers (Co/Pd, Co/Pt, Co/Cu, and Co/Ni), rare-earth and transition metal alloys, and ferromagnetic alloy/MgO bi-layers [4]–[7]. Due to its wide area of applications, permalloy ($Ni_{80}Fe_{20}$) is one of the most studied ferromagnetic materials from both theoretical and experimental point of view. It is a soft ferromagnetic alloy with a relative low Gilbert damping [8]. In this paper, we demonstrate the stabilization of PMA in MgO/$Ni_{80}Fe_{20}$/Ta multilayer stacks grown on Si/$SiO_x$ substrates, even in the as deposited state. This could be particularly interesting for complex multilayer stacks, where any annealing steps, typically involved in growing samples with PMA, would have a detrimental effect on functional properties by thermal enhancement of interfacial mixing. Moreover, this paper addresses a specific problem of the capping layer influence on the PMA. Therefore, we show here that in case of NiFe ($Ni_{80}Fe_{20}$) thin films grown on MgO underlayers, by changing the nature of the capping layer (MgO, V, Nb, Ta), we were able to stabilize or quench the PMA in the thin NiFe films.

## II. Experiment

The Si/$SiO_2$/Ta(3 nm)/MgO(1.3 nm)/NiFe(1.5–4 nm) multilayer stacks capped with V, Nb, Ta (4 nm) or with MgO(1.3 nm)/Ta(4 nm), were elaborated using a magnetron sputtering system having a base pressure lower than $4 \times 10^{-9}$ torr. The metallic films, except for the Ta capping layer, were deposited at room temperature (RT) by dc sputtering under an Ar pressure of 1 mtorr. The Ta capping layer was deposited at an Ar pressure of 5 mtorr that we optimized, for the growth of the tetragonal beta phase of Ta, by performing X-ray diffraction (XRD) experiments (not shown here). For the deposition of the NiFe layer, a 2 in $Ni_{80}Fe_{20}$ target was used. The MgO film was grown at RT by RF sputtering from a MgO polycrystalline target in an Ar pressure of 15 mtorr. After deposition, several multilayer stacks were *ex situ* annealed for 1 h at a temperature of 215 °C in a vacuum better than $5 \times 10^{-8}$ torr, in the absence of any applied magnetic field. The crystalline structure of the multilayer stacks was analyzed by XRD using a four-circle diffractometer. The magnetic properties of the films were studied at RT using a vibrating sample magnetometer.

## III. Results and Discussion

In order to determine the crystal structure of the multilayer stacks, we performed XRD experiments in grazing incidence (GI-XRD) geometry. Fig. 1 shows the diffraction pattern recorded for the Si/$SiO_2$/Ta(3 nm)/MgO(1.3 nm)/NiFe(4.5 nm)/Ta(4 nm) sample annealed at 215 °C. The XRD pattern clearly shows peaks corresponding to the Ta alpha and beta phases [9] and to the NiFe (111) and (200) reflections. The Ta alpha phase peaks are attributed to the 3 nm thick Ta seed layer, which was deposited at a lower Ar pressure of 1 mtorr. The beta phase peaks correspond to the 4 nm thick Ta capping layer. The presence of the NiFe (111) and (200) reflections indicates that NiFe film has a polycrystalline structure. After the background subtraction, the diffraction peaks were fitted using pseudo-Voigt functions. This allowed us to evaluate their full-width at half-maximum and to determine the mean structural coherence length along the grazing direction by means of the well-known Scherrer equation [10]. The obtained values are 1.4 nm for the Ta seed layer, 4 nm for the Ta capping, and a relative low value of 1.7 nm for the NiFe film.

Manuscript received March 7, 2014; revised April 11, 2014; accepted April 17, 2014. Date of current version November 18, 2014. Corresponding author: C. Tiusan (e-mail: coriolan.tiusan@phys.utcluj.ro).

Color versions of one or more of the figures in this paper are available online at http://ieeexplore.ieee.org.

Digital Object Identifier 10.1109/TMAG.2014.2320296

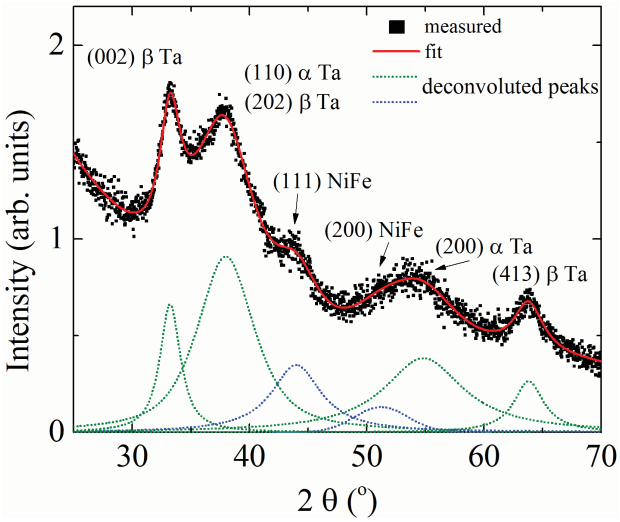


Fig. 1. XRD pattern measured in GI-XRD geometry for the Si/SiO2/Ta(3 nm)/MgO(1.3 nm)/NiFe(4.5 nm)/Ta(4 nm) multilayer stack annealed at 215 °C. Symbols: experimental data. Lines: result of the theoretical fit.

Fig. 2 shows the in-plane and out-of-plane magnetization curves for the as-deposited and the 215 °C annealed samples capped with Ta and with NiFe with nominal thicknesses of 1.3 and 1.6 nm, respectively. The 1.3 nm thick NiFe film shows PMA even before annealing. However, for samples with larger NiFe thicknesses, the PMA is lost. On the other hand, after annealing the samples, the PMA is maintained up to a nominal thickness of 1.8 nm. The inset of Fig. 2(b) shows the low field range of the hysteresis loops of the 1.6 nm annealed NiFe film, indicating a squareness ratio ($M_R/M_S$) of the out-of-plane magnetization loop close to 1.

In order to understand the effect of the capping layer on the saturation magnetization ($M_S$) of the annealed samples, we have plotted the $M_S \times t_N$ versus $t_N$ (NiFe layer nominal thickness), as illustrated in Fig. 3 for the samples capped with Ta and MgO/Ta, respectively. In this representation, the intercept with the thickness axis of the linear fit of the data gives the magnitude of the magnetic dead layer ($t_{\mathrm{DL}}$), whereas the slope gives the mean saturation magnetization of the NiFe films. These results point to the presence of a ~0.5 nm thick magnetic dead layer for the case of the NiFe films capped with MgO/Ta. Small angle X-ray reflectivity measurements (not shown here) indicated an increased roughness of the upper NiFe/MgO interface, as compares with the lower MgO/NiFe one. This result seems to suggest an increased oxidation of the upper NiFe/MgO interface, which might be responsible for the formation of the magnetic dead layer. In the case of the Ta capped samples, the magnetic dead layer thickness increases up to ~0.82 nm due to the interdiffusion at the NiFe/Ta interface. In the case of the V and Nb capping, the estimated dead layer is ~0.61 and 0.7 nm, respectively. Interestingly, the mean saturation magnetization (~800 ± 50 emu/cm$^3$) in the case of the MgO/Ta capping is consistent with the one expected for the given alloy composition (20% Fe and 80% Ni), whereas it is larger in the case of the other metallic capping layers (~970 ± 80 emu/cm$^3$ for the Ta capping). A possible mechanism explaining this behavior,

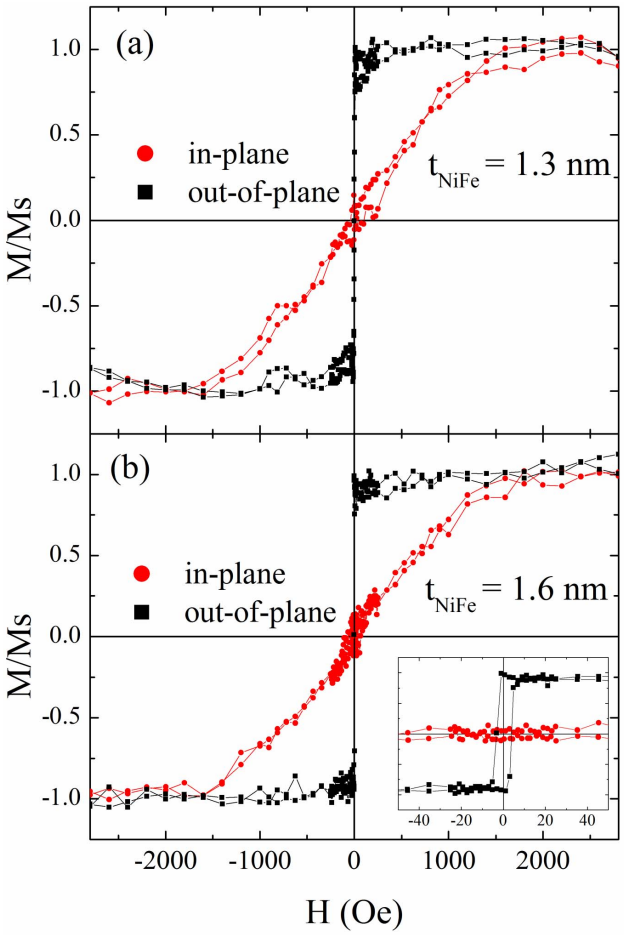


Fig. 2. In-plane and out-of-plane magnetization curves for the (a) as-deposited 1.3 nm thick NiFe film and (b) 215 °C annealed 1.6 nm NiFe film capped with Ta. Inset of (b): low field range of the hysteresis loops with squareness ratio $M_R/M_S$ around 1.

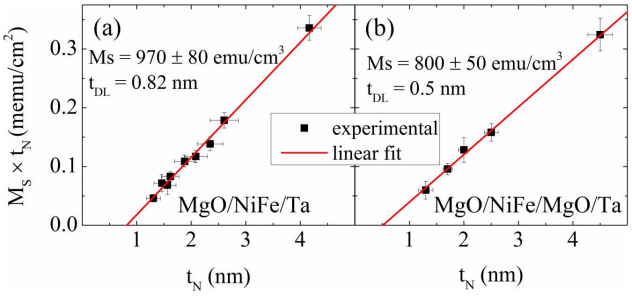


Fig. 3. $M_S \times t_N$ versus $t_N$ (NiFe layer nominal thickness) for the samples annealed at 215 °C and capped with (a) Ta and (b) MgO/Ta. The straight line is the result of the linear fit of the experimental data. The intercept with the horizontal axes represents the magnetically dead layer thickness while the slope gives the mean saturation magnetization.

which nevertheless requires further investigation, would be a preferential Ni diffusion toward the metallic capping layer. As a consequence, the local Fe concentration in the NiFe film would increase leading to an enhancement of the mean saturation magnetization.

To quantify the magnetic anisotropy in our films, the effective magnetic anisotropy constant $K_{\mathrm{eff}}$ was determined from the saturation field, $H_S$, using the relation $K_{\mathrm{eff}} = H_S M_S/2$,

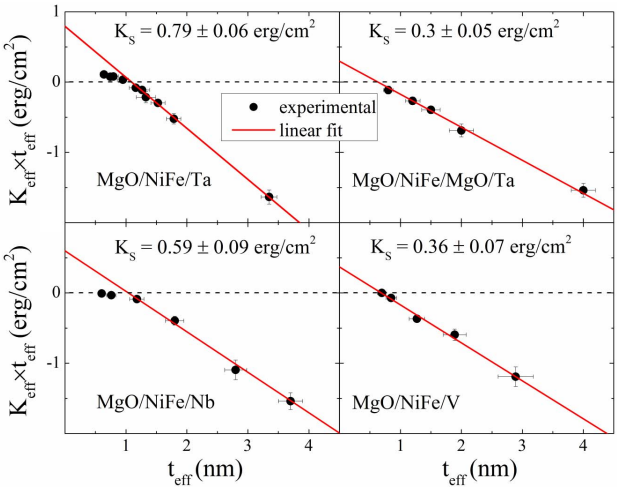


Fig. 4. $K_{\text{eff}} \times t_{\text{eff}}$ dependence on the $t_{\text{eff}}$ for the samples capped with Ta, MgO/Ta, Nb, V and annealed at 215 °C. The straight lines are the result of the linear fit of the experimental data. The intercept with the vertical axis gives the magnitude of the $K_S$.

where $M_S$ is the mean saturation magnetization. In the case of perpendicular magnetic easy axis, the $H_S$ was considered to be positive and was determined from the in-plane magnetization curve. On the other hand, in the case of in-plane magnetic easy axis, the $H_S$ was considered to be negative and was determined from the out-of-plane hysteresis loop. The $K_{\text{eff}}$ can be described by the phenomenological relation [4]

$$K_{\text{eff}} = K_V - 2\pi M_S^2 + K_S/t_{\text{eff}} \tag{1}$$

where $K_V$ describes the bulk magnetocrystalline anisotropy, $2\pi M_S^2$ is the shape anisotropy, and $K_S$ is the interface anisotropy, whereas $t_{\text{eff}} = t_N - t_{\text{DL}}$ is the effective NiFe layer thickness, which represents the width of the magnetically active layer.

From (1), by fitting the $t_{\text{eff}}$ dependence of the product $K_{\text{eff}} \times t_{\text{eff}}$ with a linear equation, the different anisotropy contributions can be evaluated, as shown in Fig. 4. For all the studied samples, the bulk anisotropy $K_V$ was found to be negligible, as expected having in view the polycrystalline nature of the NiFe films. However, the $K_S$ shows an interesting dependence on the capping layer nature, decreasing from $0.79 \pm 0.06$ erg/cm$^2$, for the Ta capping, down to $0.3 \pm 0.05$ erg/cm$^2$ in the case of the MgO/Ta capping. In the case of the Ta capping, the relative large value of the $K_S$ gives a spin reorientation transition thickness ($t_{\text{SRT}}$) of ∼1.1 nm. When the effective thickness of the NiFe layer is below $t_{\text{SRT}}$, the magnetic anisotropy easy axis switches from the in-plane to the out-of-plane direction, as in Fig. 1(b), where the effective thickness of the NiFe layer is ∼0.8 nm. In the case of the Nb capping layer, a $t_{\text{SRT}}$ of ∼1 nm can be asserted. However, the NiFe films capped with Nb with effective thicknesses below 1 nm lose their clear ferromagnetic behavior. The shape of the hysteresis curves (not shown here) for this type of films seems to suggest that the ultrathin films become super-paramagnetic, most likely, due to the decoupling of the small ferromagnetic grains. Therefore, we were unable to obtain Nb capped NiFe films showing PMA. Moreover, in the case of the MgO/Ta and V capped films an even smaller $t_{\text{SRT}}$ is obtained, ∼0.5 nm, for which the NiFe are granular in nature showing a super-paramagnetic behavior and without PMA.

In literature, the origin of PMA at 3d metal/alloy-MgO interface is commonly attributed to the hybridization of the O 2p and metal/alloy 3d orbitals [11], [12]. Therefore, as in the case of CoFeB/MgO films [13], one might expect that the sample capped with MgO/Ta to show the largest value of $K_S$ compared with the other samples with metallic capping. Nevertheless, one may clearly observe that this is not the case in our samples. This could be related to the top interface under/over oxidation influenced by the rich Ni concentration of our NiFe films [12], [14] or even stress related effects. However, to clarify this point, further studies are necessary. The MgO/Ta and V capped samples show the lowest value of $K_S$, ∼0.3 erg/cm$^2$, which increases to ∼0.59 and 0.79 erg/cm$^2$ for Nb and Ta capping, respectively. One important factor in obtaining the PMA is the degeneracy lift of the out-of-plane and in-plane 3d spin split orbitals. It has been shown [15], [16] that the d–d hybridization, between the spin-split 3d bands and the capping layer d bands with large spin-orbit (SO) interaction, generates an enhanced perpendicular orbital magnetic moment and, furthermore, through the SO coupling produces a perpendicular alignment of the spin magnetic moment. This is in agreement with our experimental observations, since the $K_S$ is increasing when changing the capping from a 3d metal (V) to a 4d (Nb) or 5d (Ta) metal, as the SO interaction increases with Z number [17]. Moreover, our experimental results supports the theoretical hypothesis issued from *ab initio* calculations [18] that the presence of a 5d transition metal monolayer over the Fe gives rise to an unexpectedly large PMA due to the large SO coupling of 5d orbitals and their hybridization with Fe 3d orbitals.

## IV. Conclusion

In this paper, we show that PMA could be achieved in $Ni_{80}Fe_{20}$ films grown on MgO underlayers, even before any annealing stages. Moreover, this paper points out the crucial role of the capping layer on the PMA stabilization. By changing the nature of the capping layer from MgO, V, Nb to Ta, the value of the surface anisotropy constant is increased in such a manner that PMA is obtained for films with an effective thickness lower than 1.1 nm. Our results demonstrate PMA in $Ni_{80}Fe_{20}$ films that are particularly important in high performance devices based on ferromagnetic films exhibiting perpendicular magnetization. Moreover, they could motivate further theoretical studies oriented toward a better understanding of mechanisms responsible on PMA stabilization.

## Acknowledgment

This work was supported in part by the POS CCE ID. 574, SMIS-CSNR 12467 Research Project, and in part by the Exploratory Research Project SPINTAIL PN-II-ID-PCE-2012-4-0315.

## References

[1] C. A. Ross, "Patterned magnetic recording media," *Annu. Rev. Mater. Res.*, vol. 31, no. 1, pp. 203–235, 2001.
[2] T. Kawahara, K. Ito, R. Takemura, and H. Ohno, "Spin-transfer torque RAM technology: Review and prospect," *Microelectron. Rel.*, vol. 52, no. 4, pp. 613–627, 2012.

[3] S. S. Parkin, M. Hayashi, and L. Thomas, "Magnetic domain-wall racetrack memory," *Science*, vol. 320, no. 5873, pp. 190–194, 2008.
[4] M. T. Johnson, P. J. H. Bloemen, F. J. A. Den Broeder, and J. J. De Vries, "Magnetic anisotropy in metallic multilayers," *Rep. Progr. Phys.*, vol. 59, no. 11, p. 1409, 1996.
[5] C. A. F. Vaz, J. A. C. Bland, and G. Lauhoff, "Magnetism in ultrathin film structures," *Rep. Progr. Phys.*, vol. 71, no. 5, p. 056501, 2008.
[6] L. E. Nistor, B. Rodmacq, S. Auffret, and B. Dieny, "Pt/Co/oxide and oxide/Co/Pt electrodes for perpendicular magnetic tunnel junctions," *Appl. Phys. Lett.*, vol. 94, no. 1, p. 012512, 2009.
[7] S. Ikeda *et al.*, "A perpendicular-anisotropy CoFeB–MgO magnetic tunnel junction," *Nature Mater.*, vol. 9, no. 9, pp. 721–724, 2010.
[8] S. Mizukami, Y. Ando, and T. Miyazaki, "Effect of spin diffusion on Gilbert damping for a very thin permalloy layer in Cu/permalloy/Cu/Pt films," *Phys. Rev. B*, vol. 66, no. 10, p. 104403, 2002.
[9] L. Ling, W. Yue, and G. Hao, "Annealing effects of tantalum films on Si and $SiO_2$/Si substrates in various vacuums," *J. Appl. Phys.*, vol. 90, no. 1, pp. 416–420, Jul. 2001.
[10] A. L. Patterson, "The Scherrer formula for X-ray particle size determination," *Phys. Rev.*, vol. 56, no. 10, pp. 978–982, 1939.
[11] H. X. Yang, M. Chshiev, B. Dieny, J. H. Lee, A. Manchon, and K. H. Shin, "First-principles investigation of the very large perpendicular magnetic anisotropy at Fe|MgO and Co|MgO interfaces," *Phys. Rev. B*, vol. 84, no. 5, p. 054401, 2011.
[12] A. Manchon *et al.*, "Analysis of oxygen induced anisotropy crossover in Pt/Co/$MO_x$ trilayers," *J. Appl. Phys.*, vol. 104, no. 4, pp. 043914-1–043914-7, Aug. 2008.
[13] H. Sato, M. Yamanouchi, S. Ikeda, S. Fukami, F. Matsukura, and H. Ohno, "Perpendicular-anisotropy CoFeB-MgO magnetic tunnel junctions with a MgO/CoFeB/Ta/CoFeB/MgO recording structure," *Appl. Phys. Lett.*, vol. 101, no. 2, pp. 022414-1–022414-4, Jul. 2012.
[14] L. E. Nistor, B. Todmacq, C. Ducruet, C. Portemont, I. L. Prejbeanu, and B. Dieny, "Correlation between perpendicular anisotropy and magnetoresistance in magnetic tunnel junctions," *IEEE Trans. Magn.*, vol. 46, no. 6, pp. 1412–1415, Jun. 2010.
[15] G. H. O. Daalderop, P. J. Kelly, and M. F. H. Schuurmans, "Magnetic anisotropy of a free-standing Co monolayer and of multilayers which contain Co monolayers," *Phys. Rev. B*, vol. 50, no. 14, p. 9989, 1994.
[16] N. Nakajima *et al.*, "Perpendicular magnetic anisotropy caused by interfacial hybridization via enhanced orbital moment in Co/Pt multilayers: Magnetic circular X-ray dichroism study," *Phys. Rev. Lett.*, vol. 81, no. 23, p. 5229, 1998.
[17] R. C. O'Handley, *Modern Magnetic Materials: Principles and Applications*. New York, NY, USA: Wiley, 1999, p. 62.
[18] D. Odkhuu, S. H. Rhim, N. Park, and S. C. Hong, "Extremely large perpendicular magnetic anisotropy of an Fe(001) surface capped by 5 d transition metal monolayers: A density functional study," *Phys. Rev. B*, vol. 88, no. 18, p. 184405, 2013.